Equation of state, fluctuations and other recent results from LQCD

2014 J. Phys.: Conf. Ser. 535 012016

(http://iopscience.iop.org/1742-6596/535/1/012016)

Journal of Physics: Conference Series **535** (2014) 012016 doi:10.1088/1742-6596/535/1/012016

Equation of state, fluctuations and other recent results from LQCD

Stefan Krieg[a,b]
for the Wuppertal-Budapest collaboration

[a]Department of Physics, University of Wuppertal,
Gaußstr. 20, D-42119, Germany
[b]Forschungszentrum Jülich, Jülich, D-52425, Germany

E-mail: s.krieg@fz-juelich.de

Abstract. We report on a continuum extrapolated result [1] for the equation of state (EoS) of QCD with $N_f = 2 + 1$ dynamical quark flavors and discuss preliminary results obtained with an addition dynamical charm quark ($N_f = 2 + 1 + 1$). Recent results on fluctuations of conserved charges (ratios of generalized susceptibilites) are reviewed and an update on crosscheck calculations using other complementary lattice actions is given. For all our final results, the systematics are controlled, quark masses are set to their physical values, and the continuum limit is taken using at least three lattice spacings corresponding to temporal extents up to $N_t = 16$.

1. Full result for the $N_f = 2 + 1$ equation of state

The rapid transition from the quark-gluon-plasma 'phase'[1] to the hadronic phase in the early universe and the QCD phase diagram are subjects of intense study in present heavy-ion experiments (LHC@CERN, RHIC@BNL, and the upcoming FAIR@GSI). This transition can be studied in a systematic way in Lattice QCD (for recent reviews see, e.g., [3, 4, 5]). The equation of state (EoS) of QCD, (i.e, the pressure p, energy density ϵ, trace anomaly $I = \epsilon - 3p$, entropy $s = (\epsilon + p)/T$, and the speed of sound $c_s^2 = dp/d\epsilon$ as functions of the temperature) has been determined by several lattice groups, however, a full result was, until recently, still lacking. Our of ref. [15] constituted a full result at three characteristic temperatures, which we have now extended to the full temperature range in [1] and made available electronically [2].

Our calculation is based on a tree-level Symanzik improved gauge action with 2-step stout-link improved staggered fermions. The precise definition of the action can be found in ref. [16], its advantageous scaling properties are discussed in ref. [8]. In particular, while it approaches the continuum value of the Stefan-Boltzmann limit in the infinite temperature limit $T \to \infty$ slower than actions with p4 or Naik terms (the latter is an additional fermionic term in the asqtad and hisq actions), it behaves monotonous and reaches the asymptotic a^2 behavior quite "early". Extrapolations from moderate temporal extents, e.g., using $N_t \geq 8$, allow for a smooth continuum extrapolation and provide an accuracy on the percent level, the typical accuracy one aims to reach. Additionally, applying simple tree-level improvement factors for the bulk

[1] Since this transition is a cross-over [6], this use of the term 'phase' is somewhat abusive, and indicates only the dominant degrees of freedom.

thermodynamic observables brings the individual data points for the different N_t very close to the continuum limit.

This points to an important advancement of the calculation described here over our previous results of [15]: we now include a large range of $N_t = 12$ data points and one $N_t = 16$ data point located at the peak position. Previously, we only had $N_t = 12$ results at three characteristic temperature values available. The $T \to 0$ limit is difficult due to taste-breaking effects, but is crucial since the renormalization is done at zero temperature, i.e. $p(T{=}0){=}0$. A mismatch at T=0 leads to a shift in the whole EoS. Previously, we calculated the difference in the pressure between the physical theory and its counterpart with 720 MeV heavy pions at a selected temperature (100 MeV), where the latter theory has practically zero pressure, and we, therefore, get $p(T = 100$ MeV) in the physical theory with the desired normalization. The difference of this result and the prediction by the Hadron Resonance Gas model (HRG) was then included in the systematical error. With our increased range of temporal extents, we now can use five lattice spacings to fix the additive term in the pressure, arriving at a complete agreement with the hadron resonance gas model at low temperatures. We also improved the precision on our line of constant physics (LCP, see ref. [1]), and used two different methods to set the scale (based on the w_0 scale [18] or on f_k) in order to control the systematical error related to scale setting.

These two different scale setting procedures entered into our 'histogram' method [19] used to estimate systematical errors, along with a range of other fit methods, each of which is an in principle completely valid approach. We then calculated the goodness of fit Q and weights based on the Akaike information criterion AICc [20, 21] and looked at the unweighted or weighted (based on Q or AICc) distribution of the results. The median is the central value, whereas the central region containing 68% of all the possible methods gives an estimate on the systematic uncertainties. This procedure provides very conservative errors. Here, we had four basic types of continuum extrapolation methods (with or without tree level improvement for the pressure and with a^2 alone or a^2 and a^4 discretization effects) and two continuum extrapolation ranges (including or excluding the coarsest lattice N_t=6 in the analysis). We used seven ways to determine the subtraction term at T=0 (subtracting directly at the same gauge coupling β or interpolating between the β values with various orders of interpolation functions), and the aforementioned two scale procedures. Finally, we had eight options to determine the final trace anomaly by choosing among various spline functions, giving altogether 4·2·7·2·8=896 methods. Note that using either an AICc or Q based distribution changed the result only by a tiny fraction of the systematic uncertainty. Furthermore, the unweighted distribution always delivered consistent results within systematical errors.

The systematic error procedure clearly demonstrates the robustness of our final result. Even in the case of applying or not applying tree level improvement, where the data points at finite lattice spacing change considerably, the agreement between the continuum extrapolated results, and hence the contribution to the systematic error, is on the few percent level.

The continuum extrapolated trace anomaly is shown in Figure 1.

The pressure is obtained via integration from the trace anomaly, see Figure 2 (left) together with the predictions of the hadron resonance gas (HRG) model at low temperatures. There is a perfect agreement with HRG in the hadronic phase. The energy and entropy densities as well as the speed of sound are shown in the right panel of Figure 2.

2. Update on the $N_f = 2 + 1 + 1$ Equation of State

So far, the equation of state is known only in 2+1 flavor QCD. The contribution from the sea charm quarks most likely matter at least for $T > 300 - 400$ MeV (for an illustration, see Figure 3).

The $N_f = 2{+}1$ lattice results of the previous section agree with the HRG at low temperatures and are correct for the small to medium temperatures, and, as is shown in Figure 3, at

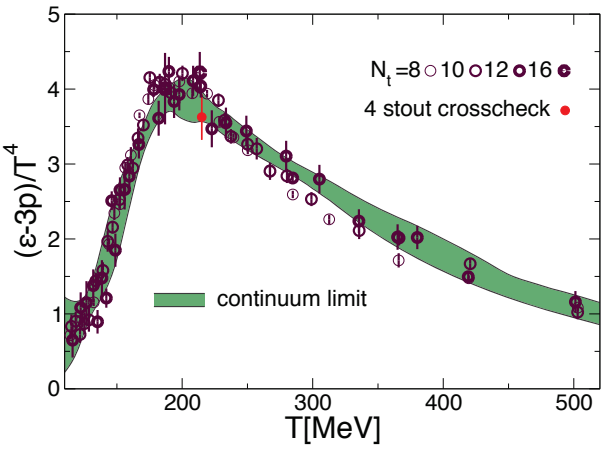

Figure 1. the trace anomaly as a function of the temperature. The continuum extrapolated result with total errors is given by the shaded band. Also shown is a cross-check point computed in the continuum limit with our new and different lattice action at $T = 214$ MeV, indicated by a smaller filled red point, which serves as a crosscheck on the peak's hight.

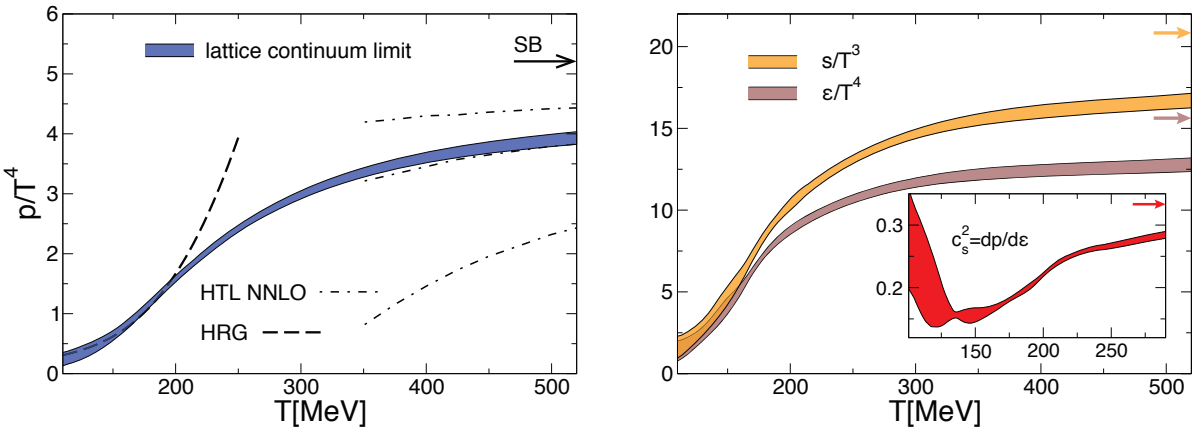

Figure 2. *Left:* continuum extrapolated result for the pressure with $N_f = 2+1$ flavors, including the HRG prediction and a comparison to the NNLO Hard Thermal Loop result of ref. [28] at high temperatures (renormalization scales $\mu = \pi T$, $2\pi T$ or $4\pi T$). *Right:* entropy and energy density. The insert shows the speed of sound.

temperatures of about 1 GeV perturbative results become sufficiently precise. Therefore, we need to calculate the EoS with a dynamical charm only for the remaining temperatures in the region of ≈ 300 MeV $< T <\approx 1000$ MeV.

As mentioned in the previous section, we are using a new lattice action for these calculations. More precisely, where our $N_f = 2+1$ calculation used an action with 2 levels of stout gauge link averaging in the coupling of the fermions to the gauge fields, we increased this to 4 levels with a smearing parameter of $\rho = 0.125$, for further details see ([1]). The crosscheck point shown in Figure 1 was computed using this new action. Since it perfectly agrees with the $N_f = 2 + 1$ results, even though it was computed using a dynamical charm, we can be certain that at temperatures at and below $T = 214$ MeV, we can rely on the $N_f = 2 + 1$ results.

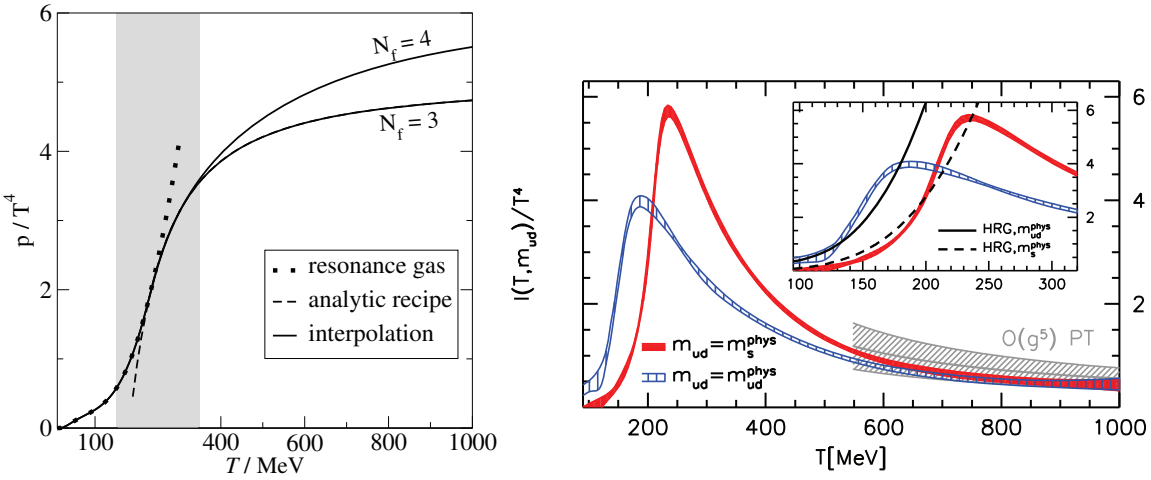

Figure 3. *Left:* Laine and Schroeder's perturbative estimate of the effect of the charm in the QCD equation of state [**?**]. *Right:* Wuppertal-Budapest [15] and perturbative (up to $O(g^5)$) results for the equation of state.

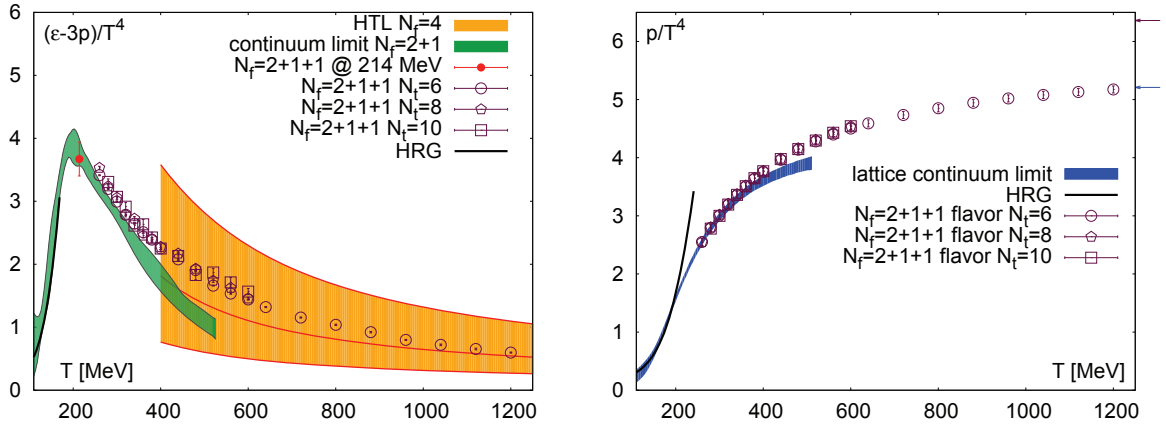

Figure 4. *Left:* Preliminary results for the charmed EoS. For comparison, we show the HRG result, the $N_f = 2+1$ band, and, at high Temperatures, the HTL result [28], where the central line marks the HTL expectation for the EoS with the band resulting from (large) variations of the renormalization scale. *Right:* Preliminary result for the pressure. All errors are statistical only.

Our preliminary results are shown in Figure 4, all errors are statistical only. Our results span a region of temperatures from $T = 214$ MeV up to $T = 1.2$ GeV. At the low end we make contact to the $N_f = 2+1$ equation of state, and at large temperatures to the HTL result. Thereby, we cover the full region of temperatures, from low temperatures, where the HRG gives reliable results, to high temperatures, where we make contact with perturbation theory. Our present set of data points will be extended to $N_t = 12$, in order to make a controlled continuum extrapolation possible.

3. Fluctuations of conserved charges and systematic uncertainties

Correlations and fluctuations of conserved charges have been proposed long ago as observables which would unambiguously signal the QCD phase transition [**?**, **?**]. The idea is that these quantum numbers have a very different value in a confined and deconfined system, and measuring them in the laboratory would allow to distinguish between the two phases. Furthermore, by directly comparing the results obtained on the lattice with those obtained by experiment, it is possible to calculate the freeze-out parameters from first principles [22, 30, 31].

Fluctuations of conserved charges can be obtained as linear combinations of diagonal and non-diagonal quark number susceptibilities, which can be calculated on the lattice at zero chemical potential [**?**, **?**]. The results we discuss here, have been obtained by our collaboration using 2+1 staggered quark flavors [**?**] with the light and strange quark masses are set to their physical values. For further details on the action and simulation setup, we refer the reader to [**?**, 22, 30, 31]. For details about the simulation algorithm we refer the reader to [8]. Here, we are mostly concerned with the systematic uncertainties of our setup.

Fluctuations of conserved charges can be computed on the lattice through generalized susceptibilities. These appear in the expansion of the QCD pressure,

$$\frac{p}{T^4} = \frac{1}{VT^3} \ln Z(V,T,\mu_B,\mu_S,\mu_Q) = \sum_{lmn} \chi^{BSQ}_{lmn} \mu_B^l \mu_S^m \mu_Q^n \tag{1}$$

with

$$\chi^{BSQ}_{lmn} = \frac{1}{VT^3} \frac{\partial^{l+m+n} \ln Z(V,T,\mu_B,\mu_S,\mu_Q)}{\partial(\mu_B/T)^l \partial(\mu_S/T)^m \partial(\mu_Q/T)^n}, \tag{2}$$

being the generalized susceptibilities. These are related to the moments of the distributions of the corresponding conserved charges by

$$\begin{aligned} \text{mean}: \ M = \chi_1 \qquad & \text{variance}: \ \sigma^2 = \chi_2 \\ \text{skewness}: \ S = \chi_3/\chi_2^{3/2} \qquad & \text{kurtosis}: \ \kappa = \chi_4/\chi_2^2 \,. \end{aligned} \tag{3}$$

With these moments we can express the volume independent ratios

$$\begin{aligned} S\sigma = \chi_3/\chi_2 \quad ; \quad & \kappa\sigma^2 = \chi_4/\chi_2 \\ M/\sigma^2 = \chi_1/\chi_2 \quad ; \quad & S\sigma^3/M = \chi_3/\chi_1 \,. \end{aligned} \tag{4}$$

We can directly compare these quantities to experiment once the experimental setting is correctly implemented: there is no strangeness input in the colliding nuclei, and the ratio of protons and neutrons in the gold or lead atoms predeterimne the charge-to-baryon ratio in the outcoming hadrons as well. Thus [**?**]:

$$\langle S \rangle = 0, \qquad \langle Q \rangle = 0.4 \, \langle B \rangle \,. \tag{5}$$

These conditions can be respected if we introduce a strange and electric charge chemical potential in addition to the baryochemical potential. In order to extract freeze-out temperature and baryon chemical potential, the ratios $S_Q\sigma_Q^3/M_Q = R^Q_{31}(T,\mu_B) = \chi^Q_3/\chi^Q_1$ (see Figure 5) and $M_Q/\sigma_Q^2 = R^Q_{12}(T,\mu_B) = \chi^Q_1/\chi^Q_2$ can be expanded (for small chemical potentials) where $\mu_Q(\mu_B)$ and $\mu_S(\mu_B)$ are chosen to satisfy Eqs. (5), see [22].

In order to obtain reliable results from the lattice, we have to perform a continuum extrapolation, with at least 3 lattice spacings. Even with these at hand, we have to insure that we are in the scaling window, as illustrated by Figure 5. In order to control the systematic

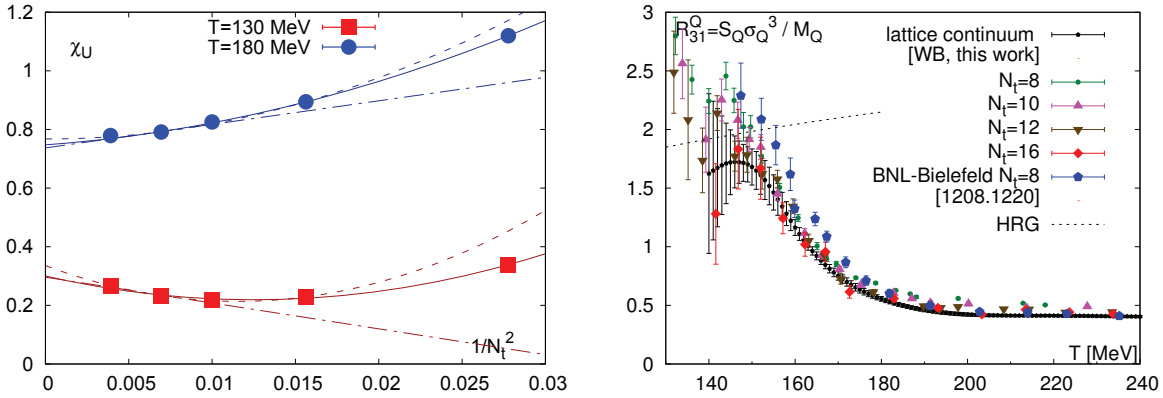

Figure 5. *Left:* χ_U, an observable severely hit both by taste breaking and by the cut-off effects in the one-link staggered dispersion relation, illustrating the need for a controlled continuum extrapolation. The data points suggest a quadratic fit in $1/N_t^2$. Here we give three possible fits both below and above the transition temperature. The solid, dashed and dash-dotted curves represent the fits on the finest five, four and three lattices, respectively. The statistical errors are much smaller than the size of the points, nevertheless the fits provide reasonable χ^2 values. *Right:* Continuum extrapolated result for $S_Q\sigma_Q^3/M_Q = R_{31}^Q$ based on $N_t = 8 \ldots 16$. For low temperatures the results agrees with the HRG expectation.

error due to the continuum extrapolation, we again follow our histogram ansatz and include several different sets of node points for our spline interpolation, extrapolate χ as well as $1/\chi$ and use different extrapolation formulae, as we did for our calculation of the EoS. We also use large N_t, as illustrated in Figure 5 and make contact with the HRG at low temperatures, where our lattice spacings are coarser.

4. Crosscheck calculations with different actions

Our results show here have all been obtained using a staggered fermion action. This and the complicated continuum limit show in Figure 5 makes crosscheck calculations using other lattice actions particularly appealing. Here, we suggest using Wilson type fermions [**?**], since they, while being considerably more expensive than staggered actions, do not suffer from taste breaking induced lattice artifacts. However, Wilson type fermions suffer from another problem, as they explicitly break chiral symmetry even at vanishing quark masses. We can improve on this problem by using the even more expensive overlap action, which has a unbroken lattice variant of chiral symmetry (which excludes operator mixing and additive quark mass renormalization exactly as the continuum action). However, at the moment simulations with overlap fermions have to be performed at fixed topological charge [**?**, 32], which will require a dedicated finite volume study in the future.

Here, we show preliminary results for two such studies, one using improved Wilson (Clover), the other using overlap type fermions. In the former case simulations include a dynamical strange quark, set to its physical value and are performed in the fixed scale approach, whereas in the latter case only two mass degenerate quark flavors are included at fixed topological charge. The results are shown in Figure 6.

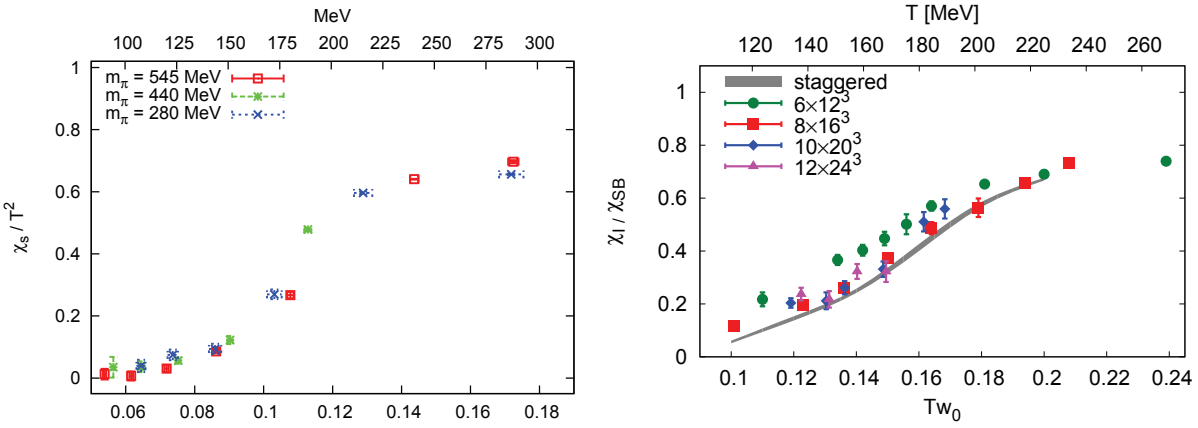

Figure 6. *Left:* Strange susceptibility at fixed lattice spacing using $N_f = 2 + 1$ flavors of Wilson (Clover) quarks, for 3 different pion masses (update of [**?**]). A chiral extrapolation and continuum limit are still pending, after which a direct comparison to staggered results will be possible. *Right:* $N_f = 2$ crosscheck calculation using overlap quarks [**?**, 32], including a dedicated $N_f = 2$ staggered calculation, all at a pion mass corresponding to about 350 MeV. The good agreement of the large N_t with the continuum extrapolated staggered result suggests that the continuum overlap and staggered results will coincide.

5. Conclusions

The precision of Lattice QCD results at finite temperature has increase significantly over the last years. We have discussed a full result (all sources of uncertainties controlled) for the $N_f = 2+1$ EoS by the Budapest-Wuppertal collaboration [1] and discussed how to include a dynamical charm quark for the $N_f = 2+1+1$ EoS and shown and discussed preliminary results. We have discussed systematic uncertainties in Lattice QCD simulations of, in particular, generalized susceptibilities and shown promising preliminary results of crosscheck calculations using other lattice actions.

Bibliography

[1] S. Borsanyi, Z. Fodor, C. Hoelbling, S. D. Katz, S. Krieg and K. K. Szabo, arXiv:1309.5258 [hep-lat].
[2] The results are available as an ancillary file to [1], where they are freely downloadable. The file contains tabulated data for the trace anomaly, pressure, entropy, energy density, and speed of sound for our temperature range.
[3] Z. Fodor and S. D. Katz, arXiv:0908.3341 [hep-ph].
[4] O. Philipsen, Prog. Part. Nucl. Phys. **70** (2013) 55 [arXiv:1207.5999 [hep-lat]].
[5] P. Petreczky, PoS ConfinementX (2012) 028 [arXiv:1301.6188 [hep-lat]].
[6] Y. Aoki, G. Endrodi, Z. Fodor, S. D. Katz and K. K. Szabo, Nature **443** (2006) 675 [hep-lat/0611014].
[7] Y. Aoki, Z. Fodor, S. D. Katz and K. K. Szabo, Phys. Lett. B **643** (2006) 46 [hep-lat/0609068].
[8] Y. Aoki, S. Borsanyi, S. Durr, Z. Fodor, S. D. Katz, S. Krieg and K. K. Szabo, JHEP **0906** (2009) 088 [arXiv:0903.4155 [hep-lat]].
[9] S. Borsanyi *et al.* [Wuppertal-Budapest Collaboration], JHEP **1009** (2010) 073 [arXiv:1005.3508 [hep-lat]].
[10] A. Bazavov, T. Bhattacharya, M. Cheng, C. DeTar, H. T. Ding, S. Gottlieb, R. Gupta and P. Hegde *et al.*, Phys. Rev. D **85** (2012) 054503 [arXiv:1111.1710 [hep-lat]].
[11] G. Endrodi, Z. Fodor, S. D. Katz and K. K. Szabo, JHEP **1104** (2011) 001 [arXiv:1102.1356 [hep-lat]].
[12] S. .Borsanyi, G. Endrodi, Z. Fodor, S. D. Katz, S. Krieg, C. Ratti and K. K. Szabo, JHEP **1208** (2012) 053 [arXiv:1204.6710 [hep-lat]].
[13] Z. Fodor and S. D. Katz, Phys. Lett. B **534** (2002) 87 [hep-lat/0104001].
[14] P. Petreczky, AIP Conf. Proc. **1520** (2013) 103.

[15] S. Borsanyi, G. Endrodi, Z. Fodor, A. Jakovac, S. D. Katz, S. Krieg, C. Ratti and K. K. Szabo, JHEP **1011** (2010) 077 [arXiv:1007.2580 [hep-lat]].
[16] Y. Aoki, Z. Fodor, S. D. Katz and K. K. Szabo, JHEP **0601** (2006) 089 [hep-lat/0510084].
[17] A. Peikert, B. Beinlich, A. Bicker, F. Karsch and E. Laermann, Nucl. Phys. Proc. Suppl. **63**, 895 (1998) [hep-lat/9709157].
[18] S. Borsanyi, S. Durr, Z. Fodor, C. Hoelbling, S. D. Katz, S. Krieg, T. Kurth and L. Lellouch *et al.*, JHEP **1209** (2012) 010 [arXiv:1203.4469 [hep-lat]].
[19] S. Durr, Z. Fodor, J. Frison, C. Hoelbling, R. Hoffmann, S. D. Katz, S. Krieg and T. Kurth *et al.*, Science **322** (2008) 1224 [arXiv:0906.3599 [hep-lat]].
[20] Hirotugu Akaike, IEEE Transactions on Automatic Control 19 (1974) 716-723
[21] C. M. Hurvich, C.-L. Tsai, Biometrika 76 (1989) 297-307
[22] S. Borsanyi, Z. Fodor, S. D. Katz, S. Krieg, C. Ratti and K. K. Szabo, Phys. Rev. Lett. **111**, 062005 (2013) [arXiv:1305.5161 [hep-lat]].
[23] S. .Borsanyi, G. Endrodi, Z. Fodor, S. D. Katz and K. K. Szabo, JHEP **1207** (2012) 056 [arXiv:1204.6184 [hep-lat]].
[24] G. Endrodi, Z. Fodor, S. D. Katz and K. K. Szabo, PoS LAT **2007** (2007) 228 [arXiv:0710.4197 [hep-lat]].
[25] P. Petreczky [for HotQCD Collaboration], PoS LATTICE **2012** (2012) 069 [arXiv:1211.1678 [hep-lat]].
[26] P. Huovinen and P. Petreczky, Nucl. Phys. A **837**, 26 (2010) [arXiv:0912.2541 [hep-ph]].
[27] S. Borsanyi, G. Endrodi, Z. Fodor, S. D. Katz, S. Krieg, C. Ratti, C. Schroeder and K. K. Szabo, PoS LATTICE **2011** (2011) 201 [arXiv:1204.0995 [hep-lat]].
[28] J. O. Andersen, L. E. Leganger, M. Strickland and N. Su, JHEP **1108** (2011) 053 [arXiv:1103.2528 [hep-ph]].
[29] G. I. Egri, Z. Fodor, C. Hoelbling, S. D. Katz, D. Nogradi and K. K. Szabo, Comput. Phys. Commun. **177** (2007) 631 [hep-lat/0611022].
[30] S. Borsanyi, Z. Fodor, S. D. Katz, S. Krieg, C. Ratti and K. K. Szabo, arXiv:1403.4576 [hep-lat].
[31] C. Ratti, these proceedings.
[32] S. Borsanyi, Y. Delgado, S. Drr, Z. Fodor, S. D. Katz, S. Krieg, T. Lippert, D. Nogradi, K. K. Szabo, B. C. Toth, PoS(LATTICE 2013) 163